Sigma 1 Receptor Modulates Optic Nerve Head Astrocyte Reactivity

Jing Zhao,[1,3] Graydon Gonsalvez,[2] Manuela Bartoli,[2,3] Barbara A. Mysona,[1–3] Sylvia B. Smith,[1–3] and Kathryn E. Bollinger[1–3]

[1]Department of Ophthalmology, Medical College of Georgia at Augusta University, Augusta, Georgia, United States
[2]Department of Cellular Biology and Anatomy, Medical College of Georgia at Augusta University, Augusta, Georgia, United States
[3]Culver Vision Discovery Institute, Augusta, Georgia, United States

Correspondence: Kathryn E. Bollinger, Cellular Biology and Anatomy, 1120 15th St BA 2701, Augusta, GA 30912, USA; kbollinger@augusta.edu.

Received: November 26, 2020
Accepted: May 3, 2021
Published: June 4, 2021

Citation: Zhao J, Gonsalvez G, Bartoli M, Mysona BA, Smith SB, Bollinger KE. Sigma 1 receptor modulates optic nerve head astrocyte reactivity. *Invest Ophthalmol Vis Sci.* 2021;62(7):5. https://doi.org/10.1167/iovs.62.7.5

Purpose. Stimulation of Sigma 1 Receptor (S1R) is neuroprotective in retina and optic nerve. S1R is expressed in both neurons and glia. The purpose of this work is to evaluate the ability of S1R to modulate reactivity responses of optic nerve head astrocytes (ONHAs) by investigating the extent to which S1R activation alters ONHA reactivity under conditions of ischemic cellular stress.

Methods. Wild type (WT) and S1R knockout (KO) ONHAs were derived and treated with vehicle or S1R agonist, (+)-pentazocine ((+)-PTZ). Cells were subjected to six hours of oxygen glucose deprivation (OGD) followed by 18 hours of re-oxygenation (OGD/R). Astrocyte reactivity responses were measured. Molecules that regulate ONHA reactivity, signal transducer and activator of transcription 3 (STAT3) and nuclear factor kappa B (NF-kB), were evaluated.

Results. Baseline glial fibrillary acidic protein (GFAP) levels were increased in nonstressed KO ONHAs compared with WT cultures. Baseline cellular migration was also increased in nonstressed KO ONHAs compared with WT. Treatment with (+)-PTZ increased cellular migration in nonstressed WT ONHAs but not in KO ONHAs. Exposure of both WT and KO ONHAs to ischemia (OGD/R), increased GFAP levels and cellular proliferation. However, (+)-PTZ treatment of OGD/R-exposed ONHAs enhanced GFAP levels, cellular proliferation, and cellular migration in WT but not KO cultures. The (+)-PTZ treatment of WT ONHAs also enhanced the OGD/R-induced increase in cellular pSTAT3 levels. However, treatment of WT ONHAs with (+)-PTZ abrogated the OGD/R-induced rise in NF-kB(p65) activation.

Conclusions. Under ischemic stress conditions, S1R activation enhanced ONHA reactivity characteristics. Future studies should address effects of these responses on RGC survival.

Keywords: astrocytes, optic nerve head, hypoxia, neuroprotection

Astrocytes are the most abundant cells in the optic nerve head (ONH), and the ONH is an important site for early damage in glaucoma, the leading cause of irreversible blindness in the world.[1–3] Therefore responses of optic nerve head astrocytes (ONHAs) to physiological and pathological conditions within the ONH, and effects of these responses on neighboring RGC axons, are critically important. For example, in glaucomatous models in mice and rats, ONHAs undergo reactive changes.[4–6] These include proliferation, migration, gene expression changes, upregulation of glial fibrillary acidic protein (GFAP), and extension of longitudinal processes.[5,7–10] In addition, studies performed in an experimental rat glaucoma model indicate that ONH astrocytes undergo actin cytoskeletal changes that occur before microtubule-based RGC axonal reorganization.[5] Although glaucoma-associated astrocyte reactivity is not well understood, studies suggest that aspects of ONHA response to glaucomatous stress are protective of RGCs.[11] This glia-mediated neuroprotection was attenuated in the absence of the critical astrocyte reactivity regulator, STAT3, using a unilateral induced mouse model of glaucoma.[12]

Onset and progression of glaucomatous optic neuropathy are closely associated with intraocular pressure.[13–15] However, studies in human patients and in nonhuman primate models of experimental glaucoma indicate that abnormal autoregulation of optic nerve head blood flow also plays a role in the pathogenesis of this and other optic neuropathies.[16–22] Alterations in blood flow to the optic nerve head include episodes of transient ischemia followed by reperfusion. Studies indicate that subjecting ONHAs to periods of ischemia/reperfusion stress enhances characteristics of astrocyte reactivity.[23] In this study, we aimed to evaluate the effects of Sigma 1 receptor (S1R) activation and inhibition on ONHA reactivity responses under conditions of oxygen glucose deprivation and reperfusion (OGD/R).

S1R is a unique transmembrane protein that is expressed in neuronal and glial cell types throughout the central and peripheral nervous systems, including the optic nerve

head.[24–26] S1R is considered a potential therapeutic target for neurological pathologies including Alzheimer's and Parkinson's diseases, amyotrophic lateral sclerosis, and ischemic stroke.[27–31] In addition, recent studies support the benefit of targeting S1R in retinal and optic nerve disorders that affect both photoreceptors and ganglion cells.[32] For example, RGC loss was attenuated by administration of an S1R agonist in a rat model of ischemia-reperfusion retinopathy, and models of diabetic retinopathy and NMDA-induced inner retinal toxicity.[33–37] In addition, photoreceptor cell loss was mitigated using the S1R agonist, (+)-pentazocine ((+)-PTZ), in an inherited mouse model of retinal degeneration, and in a model of light-induced retinopathy.[38,39] Furthermore, multiple investigations of S1R knockout animals have documented accelerated neurodegenerative pathology in the brain, spinal cord and retina when S1R is absent.[27,40–42]

Because S1R is expressed in both neurons and glia, mechanistic evaluations of its neuroprotective effects have involved both cell types. Relevant to the optic nerve head, evaluations of isolated primary RGCs show (+)-PTZ-mediated neuroprotection under conditions of metabolic, excitotoxic, and ischemic cellular stress.[43–45] In addition, our previous studies of ONHAs indicate that activation of S1R using (+)-PTZ mitigates generation of intracellular reactive oxygen species and protects ONHAs from oxidative stress-induced cell death.[46] Whether simply promoting survival of ONHAs contributes to or detracts from protection of neighboring RGCs is not known. However, astrocyte reactivity has recently been correlated with RGC survival under conditions of glaucomatous stress.[12] Therefore we undertook studies to evaluate whether stimulation of S1R caused changes in basic properties of astrocyte reactivity at baseline and under conditions of ischemic cellular stress. In addition, we evaluated the effects of the S1R-specific agonist, (+)-PTZ, on activation of major astrocyte reactivity regulators, STAT3, and NFkB.

Methods and Materials

Primary Mouse Optic Nerve Head Astrocytes (ONHAs) Culture

Experiments requiring animals adhered to the ARVO Statement for the Use of Animals in Ophthalmic and Vision Research. Our animal protocol is approved by Augusta University Institutional Animal Care and Use Committee (2011-0338). Adult primary mouse optic nerve head astrocytes were isolated from optic nerve heads of C57BL/6J mice (WT) (The Jackson Laboratory, Bar Harbor, ME, USA) and S1R knockout (S1R KO) (see Wang et al.[47]) mice according to our previously published protocol for young rats with minor variations.[46] Briefly, six-week-old mice were euthanized. Six mice were used for each cell culture experiment. Optic nerve head tissue was dissected proximal to the sclera and was digested for 15 minutes using 0.05% trypsin (Invitrogen, Carlsbad, CA, USA) at 37°C. Optic nerve heads were washed once with ONHAs growth media (Dulbecco's modified Eagle's medium [DMEM]/F12 (Invitrogen) containing 10% of fetal bovine serum (FBS) (Atlanta Biologicals, Atlanta, GA, USA), 1% penicillin/streptomycin (Invitrogen), 1% Glutamax [Invitrogen], and 25 ng/mL epidermal growth factor [Sigma-Aldrich Corp., St. Louis, MO, USA]), and spun for five minutes at 2000 rpm. Optic nerve heads were resuspended in ONHA growth media and plated on 0.2% gelatin (Sigma-Aldrich Corp.) coated T75 cell-culture flasks. ONH astrocytes emerged from the ONHs after five days. ONHAs were maintained in a humidified incubator containing 5% CO_2 at 37°C. Cells were passaged after seven to 10 days and were used at passages 2 to 5. Immunocytochemistry and Western blot analyses were performed to verify the purity of ONHA cultures.

Oxygen-Glucose Deprivation/Reoxygenation (OGD/R)

Mouse ONHAs were washed twice with glucose-free DMEM (Invitrogen) containing 10% FBS and 1% penicillin/streptomycin (OGD medium), then placed into a hypoxia chamber filled with a gas mixture of 94.5%N_2/0.5%O_2/5% CO_2 at 37°C. After six hours of OGD, media was changed to DMEM with 1 g/L glucose containing 10% FBS and 1% penicillin/streptomycin (reperfusion medium) for an additional 18 hours of reoxygenation in standard incubation conditions. ONHA control cells were maintained in reperfusion media for 24 hours at standard incubator conditions.

Cell Culture Treatment Optimization

ONHAs were exposed to increasing (+)-(PTZ) (Sigma-Aldrich Corp.) concentrations (1, 3, 10, 20, 50 µM) for 24 hours in reperfusion medium to determine effects of (+)-PTZ on ONHA viability, GFAP, and S1R levels. OGD exposure times were tested with and without reoxygenation to evaluate effects of OGD on ONHA reactivity. For OGD experiments in this study, ONHAs were pretreated with 10 µM PTZ for one hour followed by six hours of OGD and an additional 18 hours of reoxygenation.

Immunocytochemistry

Cells were fixed with 4% paraformaldehyde (Electron Microscopy Sciences, Hatfield, PA) at room temperature for 15 minutes, followed by washing with PBS three times. Cells were then membrane-permeabilized with 0.3% triton X-100 in PBS at room temperature for 10 minutes. Next, cells were blocked with 0.1% triton X-100 in PBS (PBST) with 10% goat serum (Sigma-Aldrich Corp.) at room temperature for one hour, then incubated in primary antibody (glial fibrillary acidic protein [GFAP] 1:500, Dako, Carpinteria, CA, USA; Iba-1 1:500, Wako, Richmond, VA, USA; oligodendrocyte-specific protein (OSP) 1:500, Abcam, Cambridge, MA, USA; S1R 1:500; Arp3 1:100, Abcam) at 4°C overnight. The S1R rabbit polyclonal antibody was raised from peptide sequence SEVYYPGETVVHGPGEATDVEWG (corresponds to residues 143–165 of rat S1R) and generated within the laboratory of Dr. Sylvia Smith.[34] This antibody has been used in numerous publications since 2002 as a tool for study of S1R expression and function. On the second day, cells were incubated in secondary antibody (Alexa Fluor 555–labeled goat anti rabbit 1:1000; Invitrogen) at room temperature for two hours. After washing three times with PBST, coverslips were mounted with Fluoroshield with DAPI (Sigma-Aldrich Corp.). Cells were observed for immunofluorescence using a Zeiss Axioplan-2 microscope (Carl Zeiss, Oberkochen, Germany) equipped with AxioVision program (version 4.6.3) and a high-resolution microscopy camera. Mean signal intensity was determined by quantifying integrated density for each microscope field and then dividing

Investigative Ophthalmology & Visual Science

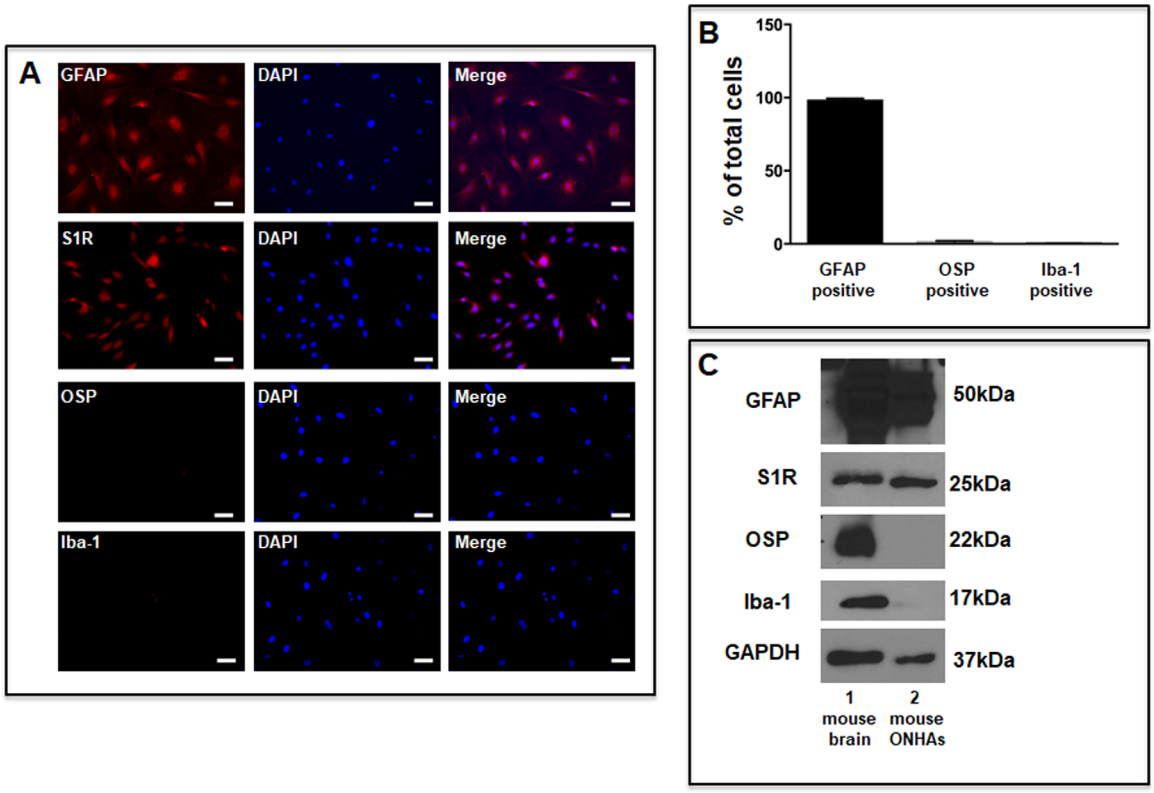

Figure 1. Characterization of cultured primary mouse ONHAs. (**A**) ONHAs were fixed and probed with antibodies against GFAP (*red*), S1R (*red*), OSP (*red*), and Iba-1 (*red*). The cells were counterstained with DAPI to label DNA (*blue*) as a marker for nuclei. *Scale bar*: 50 µm. (**B**) Quantitative analysis shows that more than 95% of the cells in culture express GFAP. (**C**) The cell lysates from ONHAs (lane 2) were positive for GFAP, a marker for astrocytes and S1R, but negative for Iba-1, a marker for microglial cells, and OSP, a marker for oligodendrocytes. The protein extract from mouse brain (lane 1) was used as positive controls. Analyses were repeated in duplicate with cells isolated from different dates, different animals and treated on different days. For each immunofluorescence evaluation, three coverslips were quantified per group. Iba-1 is a marker for microglial cells.

by the number of cells per field. For the lamellipodia staining, cells were fixed and permeabilized as described above. After blocking, cells were incubated with the Arp3 antibody (1:100; Abcam) overnight at 4°C. The next day, the coverslips were washed with PBST and incubated with secondary antibody (goat anti-mouse Alexa 555, 1:1000; Invitrogen) and Alexa488-conjugated Phalloidin (1:50; Invitrogen). The cells were then washed with PBST, counterstained with DAPI, and imaged. Images for this experiment were captured on a Leica Stellaris inverted confocal microscope (Leica, Wetzlar, Germany). Arp3-positive cellular protrusions located at the wound edge were scored as lamellipodia. Individual cells were identified using DAPI nuclear stain and the number of lamellipodia per wound edge cell were counted. One hundred cells were scored per condition.

Western Blot Analysis

Mouse optic nerve head astrocytes were lysed in RIPA buffer (Sigma-Aldrich Corp.) containing 2 mM sodium orthovanadate and 1% protease inhibitor cocktail (Thermo Scientific, Waltham, MA, USA). Cell lysates were centrifuged at 14,000*g* for 30 minutes. Protein concentration was measured by Bradford assay (Bio-Rad, Hercules, CA, USA). Proteins were separated by electrophoresis on a 4% to 15% SDS-polyacrylamide gel, and then transferred to a nitrocellulose membrane (Thermo Scientific). The membrane was blocked with 5% nonfat milk in Tris-buffered saline solution–0.05% Tween 20 for one hour at room temperature, then incubated overnight at 4°C with primary antibodies (GFAP 1:1000; Iba-1 1:500; OSP 1:1000; S1R 1:1000; glyceraldehyde-3-phosphate dehydrogenase [GAPDH] 1:2000; pSTAT3 1:500; STAT3 1:500, p-p65 1:500). After three washes in Tris-buffered saline solution–0.05% Tween 20, the membrane was incubated for 1h with an appropriate Horseradish Peroxidase (HRP)-conjugated secondary antibody at room temperature. Proteins were visualized by incubating with a SuperSignal West Pico chemiluminescent substrate (Thermo Scientific) and quantified by densitometry with ImageJ software (http://imagej.nih.gov/ij/; provided in the public domain by the National Institutes of Health, Bethesda, MD). Blots were stripped and reprobed for loading controls. GFAP antibody was purchased from Dako; Iba-1 antibody from Wako; OSP antibody from Abcam; pSTAT3, STAT3 and p-p65 antibodies from Cell Signaling Technology, Danvers, MA, USA; GAPDH monoclonal antibody, HRP-conjugated anti-rabbit IgG, and HRP-conjugated anti-mouse IgG from Santa Cruz Biotechnology, Dallas, TX, USA.

MTT Assay

C57BL/6J and S1R KO mouse optic nerve head astrocytes were seeded onto 96-well plates at a density of 10,000 cells/well in ONHA reperfusion media. After incubation

Investigative Ophthalmology & Visual Science

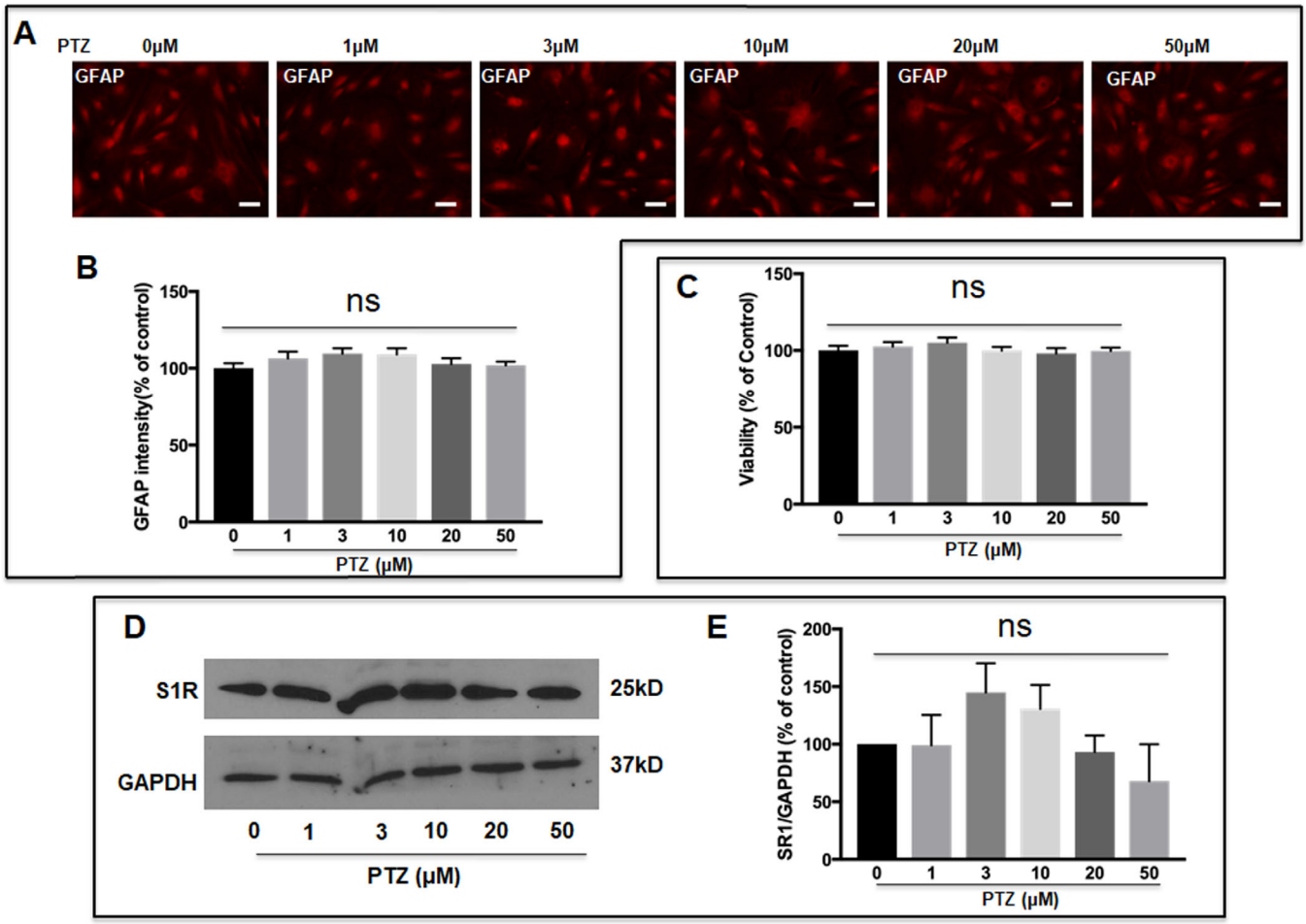

Figure 2. Effect of (+)-PTZ on WT ONHA viability, GFAP and S1R expression. WT ONHAs were treated with (+)-PTZ at varying concentrations (1, 3, 10, 20, or 50 μM) for 24 hours. (**A**) Representative images of GFAP expression detected by immunocytochemistry using GFAP antibody. *Scale bar*: 50 μm. (**B**) Quantification of GFAP staining intensity showed no significant differences with varying (+)-PTZ concentrations. (**C**) MTT assay showed no significant differences in ONHA viability with varying (+)-PTZ concentrations. (**D**) S1R expression was detected by Western blot and (**E**) quantified relative to GAPDH. No significant differences in S1R expression with varying (+)-PTZ concentrations were detected. Analyses were repeated in triplicate with cells isolated from different dates, different animals and treated on different days. For GFAP expression experiments, three coverslips were quantified from each group of each isolation. Eight microscopic fields were quantified per coverslip.

at standard conditions with increasing concentrations of S1R ligands for 24 hours, medium was removed and MTT (1.2 mM in reperfusion medium) (Invitrogen) was added and incubated for four hours at 37°C. Solubilization with dimethyl sulfoxide (Sigma-Aldrich Corp.) was performed according to protocol directions. Absorbance was measured at 540 nm using a microplate reader (VERSA max; Molecular Devices, Sunnyvale, CA, USA).

Migration (Wound-Healing) Assay

ONHAs were seeded on coverslips in 24-well plates. The next day, cells were pretreated with or without 10 μM (+)-PTZ for one hour. Cell-containing coverslips were manually scratched with a 200-μL pipet tip in an X-pattern followed by two PBS washes. Baseline cell-seeded, scratched coverslips were fixed immediately after scratching to quantify the standard scratch width. The remaining scratched coverslips were cultured for 24 hours, then washed, fixed and stained for GFAP and DAPI. For ONHA migration under OGD conditions, ONHAs were pretreated with or without 10 μM (+)-PTZ for one hour followed by scratching and culture in OGD media, with or without 10 μM (+)-PTZ, for six hours. After this, the scratched cells were subjected to 18 hours of reoxygenation in reperfusion media, with or without 10 μM (+)-PTZ. At experiment end, cells were fixed and stained with GFAP antibody and DAPI and then imaged. Eight equal area images of the scratch were taken for each coverslip. The average of baseline scratch width measurements provided the standard scratch width. For all experimental coverslips, cells inside the standard scratch width were counted as migrated cells. For each condition, the number of migrated cells was the average of cell migration counts over the eight equal area images of each coverslip. Each experiment was repeated three times.

Statistical Analysis

Data for MTT assay, immunocytochemistry and Western blot were analyzed using *t*-test, one- or two-way ANOVA, followed by Tukey-Kramer post hoc test for multiple

Investigative Ophthalmology & Visual Science

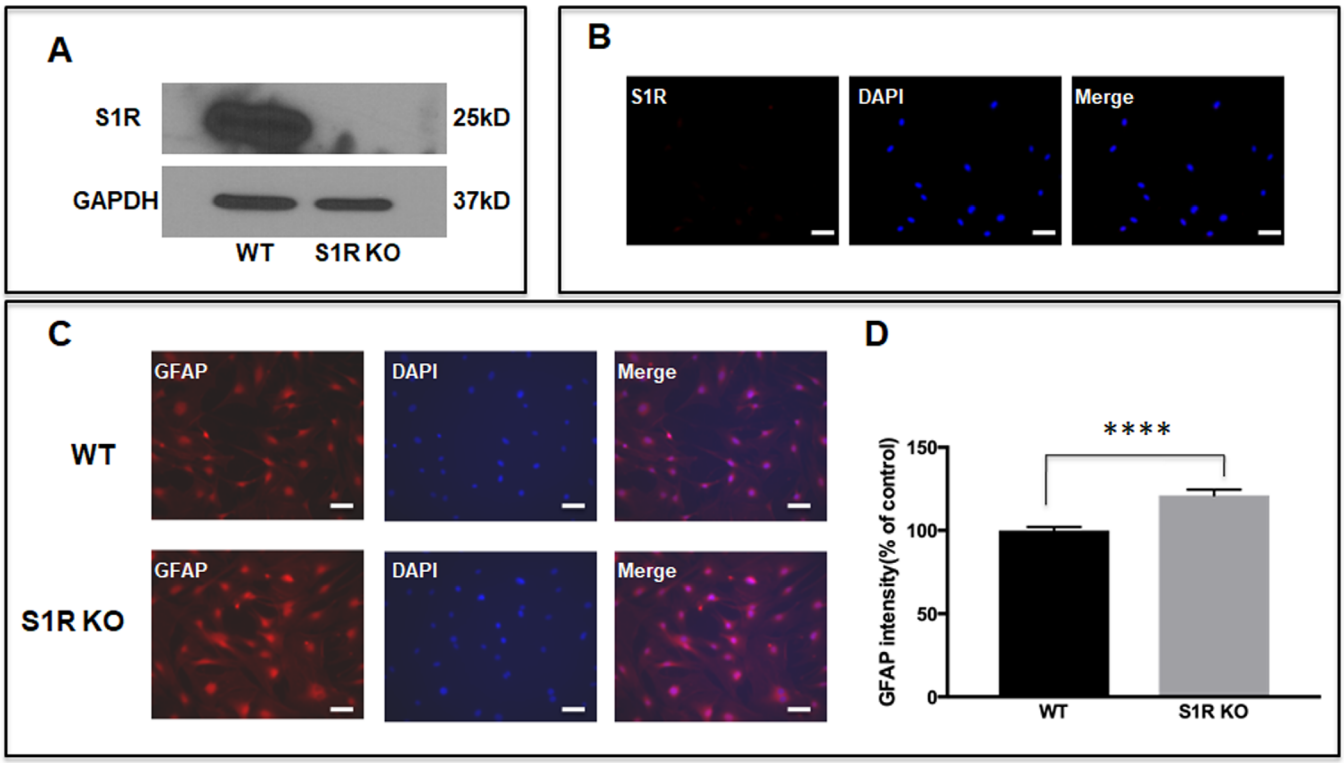

Figure 3. GFAP expression in Sigma 1 Receptor knock out (S1R KO) ONHAs. (**A**) Western analysis showed that ONHAs isolated from S1R KO mice lacked S1R. (**B**) Immunocytochemistry showed that ONHAs isolated from S1R KO mice lacked S1R. Both WT and S1R KO ONHAs were plated on coverslips and incubated for 24 hours. (**C**) Representative images show cells stained with GFAP antibody. *Scale bar*: 50 µm. (**D**) S1R KO ONHAs expressed higher GFAP than WT ONHAs under the same cell culture conditions. These results were repeated five times with cells isolated from different dates, different animals and treated on different days. For each group of each isolation, three coverslips were quantified. Significantly different from control ****$P < 0.0001$. Data were analyzed using Student's *t*-test.

comparisons. Significance was set at $P < 0.05$ (Prism; GraphPad Software, Inc. La Jolla, CA, USA).

Results

Previous work indicates that S1R is expressed in RGCs and glial cells of the optic nerve.[26,46] In addition, we have found S1R to be present within primary cultures of ONHAs derived from neonatal rat optic nerve heads.[46] To evaluate responses of mature ONHAs in the presence and absence of S1R, the current studies used primary cultures derived from adult WT C57BL6 and S1R KO C57BL6 mice. Immunocytochemical and Western blot evaluation of cultured cells showed expression of both S1R and the astrocytic marker, GFAP (Figs. 1A, 1C). Quantitative analysis of immunocytochemistry results revealed that >95% of cells in culture expressed GFAP (Fig. 1B). Cell cultures were also evaluated using immunocytochemistry and Western blot analyses for expression of ionized calcium binding adaptor molecule 1 (Iba-1), a marker of microglia, and oligodendrocyte-specific protein (OSP-1), a marker of oligodendrocytes. Representative immunocytochemistry images shown in Figure 1A and western blot analysis shown in Figure 1C indicate absence of both microglia (Iba-1) and oligodendrocyte (OSP-1) markers. Thus, we verified the purity of our isolated, cultured WT and KO ONHAs was acceptable and proceeded with cell culture experiments.

To evaluate whether baseline stimulation of S1R leads to changes in properties of ONHA reactivity, we subjected ONHAs to increasing dosages of (+)-PTZ (1-50 µM). We chose this concentration range, as shown in Figure 2, because previous reports described (+)-PTZ-mediated cytoprotection of both glial and neuronal cultures within these dosages.[43,46] We then used immunocytochemistry to evaluate intracellular levels of GFAP, a cytoskeletal protein known to be associated with increased reactivity.[48] Under baseline conditions, in the absence of induced cellular stress, we found no change in intracellular GFAP levels when WT ONHAs were exposed to increasing dosages of (+)-PTZ (Figs. 2A, 2B). Results also showed that these doses of (+)-PTZ did not affect cell viability (Fig. 2C). In addition, results showed no significant difference in S1R levels derived from (+)-PTZ–treated WT ONHAs (Figs. 2D, 2E). For subsequent experiments, we chose to use a 10 µM concentration of (+)-PTZ because this dosage of (+)-PTZ has been shown to attenuate oxidative stress and promote survival of ONHAs in culture.[46]

To evaluate the effects of S1R deletion on ONHAs, we isolated primary cultures from S1R KO mice (Figs. 3A, 3B). Both Western blot analysis of S1R levels in astrocyte cell lysates and immunocytochemical evaluation of cell cultures confirmed that ONHAs derived from KO animals lacked S1R (Figs. 4A, 4B). Next, both WT and S1R KO ONHAs were cultured for 24 hours under baseline conditions in the absence of induced cellular stress. Baseline GFAP levels were

Investigative Ophthalmology & Visual Science

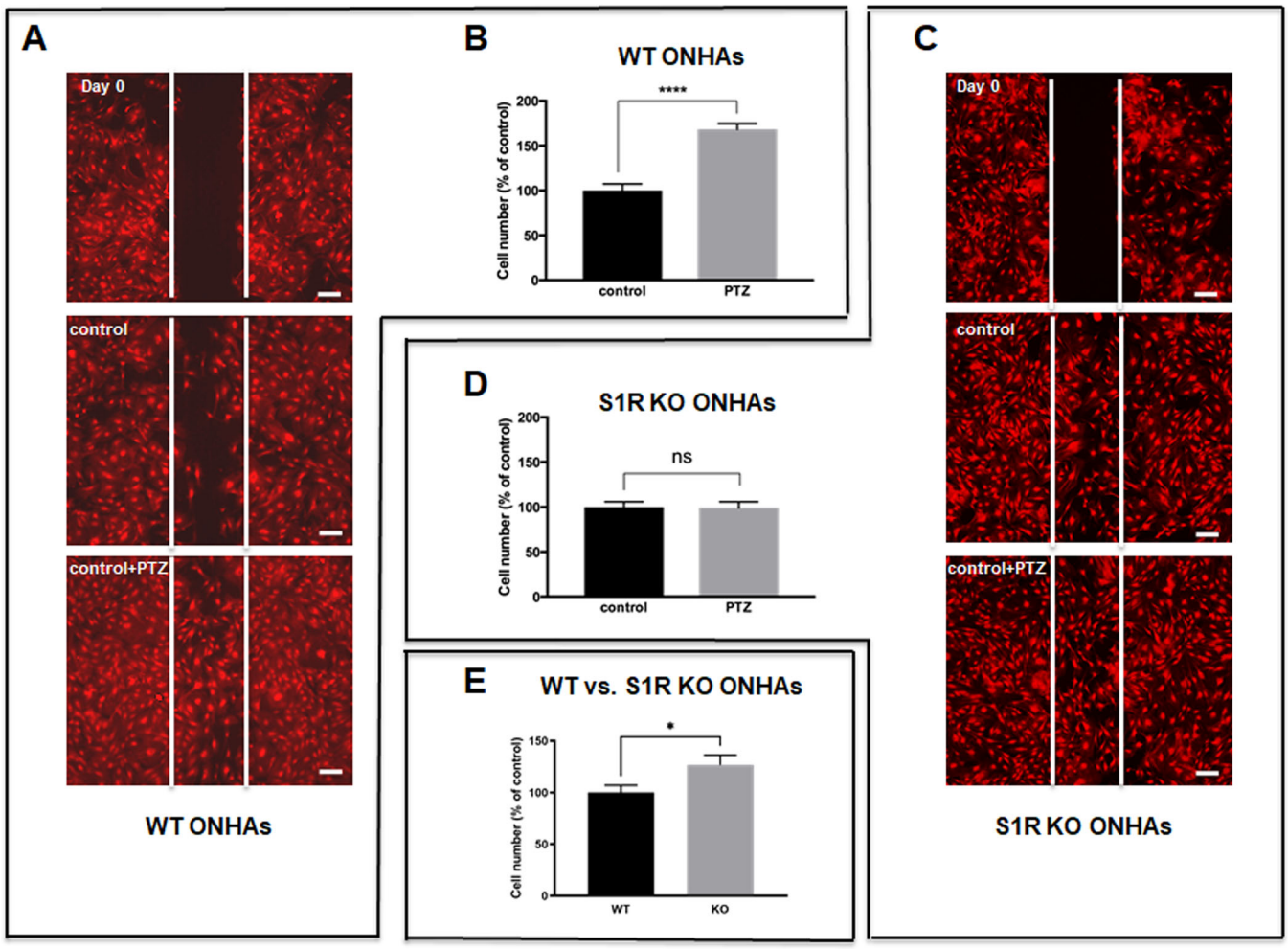

Figure 4. Effect of (+)-PTZ on WT and S1R KO ONHA migration. WT and S1R KO ONHAs were pretreated with 10 µM (+)-PTZ or vehicle for 1h before scratching. After scratching, the cells were incubated with 10 µM (+)-PTZ or vehicle for 24 hours. (**A**) Representative images show the original scratch (day 0), and migration of WT ONHAs into the wound area after 24 hours of incubation with (+)-PTZ treatment or vehicle control. *Scale bar*: 200 µm. (**B**) Quantification of the number of WT ONHAs migrated into the wounded (scratched) area. Cells in wounded area were counted using ImageJ. For each group, four coverslips were quantified. WT ONHA migration increased significantly when cells were treated with (+)-PTZ. Significantly different from control ****$P < 0.0001$. (**C**) Representative images show the original scratch (day 0) and migration of KO ONHAs into the wound area after 24 hours of incubation with (+)-PTZ treatment or vehicle control. *Scale bar*: 200 µm. (**D**) Quantification of the number of KO ONHAs migrated into the wounded (scratched) area. Cells in wounded area were counted by ImageJ. For each group, three coverslips were quantified. (+)-PTZ did not affect S1R KO ONHA migration. (**E**) S1R KO control ONHAs had significantly more migrated cells than WT control ONHAs. Significantly different from control *$P < 0.05$. Data were analyzed using Student's *t*-test. These results were repeated in triplicate with cells isolated from different dates, different animals and treated on different days. For each group of each isolation, three coverslips were quantified.

compared between WT and KO cultures using immunocytochemistry (Fig. 3C). We found significantly higher baseline levels of GFAP in nonstressed, KO-derived ONHAs compared with nonstressed, WT-derived cultures (Figs. 3C, 3D).

In addition to upregulation of cytoskeletal proteins, reactive astrocytes undergo a series of functional changes, including increased migration.[49] To determine whether stimulation of S1R would influence migration, we evaluated extent of ONHA migration using a scratch wound assay. WT ONHAs were pretreated with either 10 µM (+)-PTZ or vehicle (control) for one hour before scratch and continued either (+)-PTZ or vehicle treatment for 24 hours after scratch. Figure 4A shows representative images. Compared with the vehicle-treated (control) group, astrocyte migration into the wound area was significantly increased in the (+)-PTZ treated WT cultures (Figs. 4A, 4B).

To determine whether S1R was required for (+)-PTZ–mediated enhancement of ONHA migration, we evaluated cellular migration in (+)-PTZ–treated KO ONHA cultures. Cultured KO ONHAs were treated with either 10 µM (+)-PTZ or with vehicle (control) for one hour before scratch. This treatment, with either (+)-PTZ or vehicle, was continued for 24 hours after scratch. In contrast to the (+)-PTZ–induced increase in astrocyte migration observed in WT-derived ONHAs (Figs. 4A, 4B), we found no (+)-PTZ–induced migration enhancement in KO-derived cultures (Figs. 4C, 4D).

In addition, we compared the baseline migration level of non-stressed, nontreated, KO-derived ONHAs to nonstressed, nontreated, WT derived cultures. Our results showed significantly increased migration in KO-derived ONHAs compared with WT cells (Fig. 4E). Thus, although

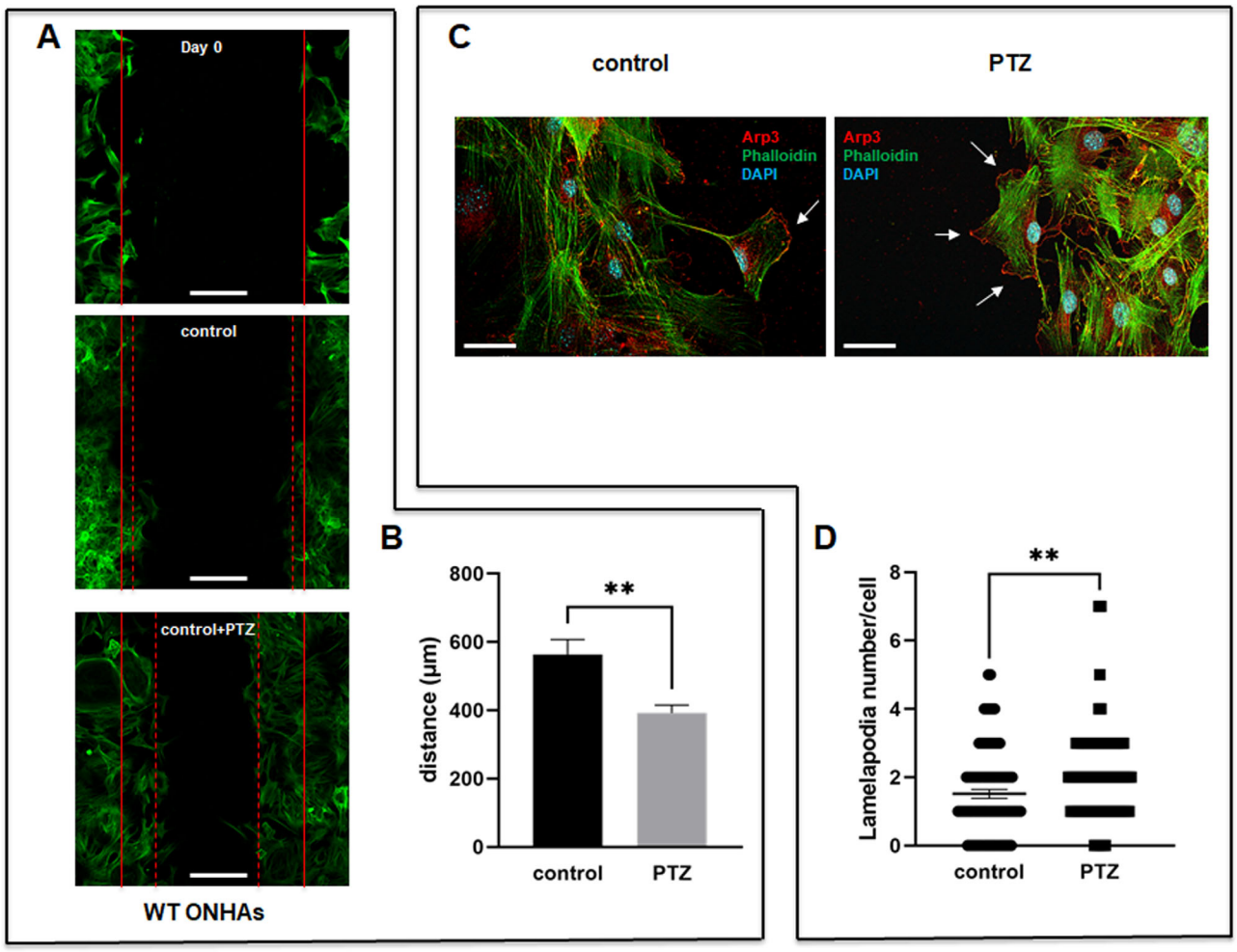

Figure 5. Effect of (+)-PTZ on WT ONHAs migration after five hours of treatment and on lamellipodia marker expression. WT ONHAs were pretreated with 10 µM (+)-PTZ or vehicle for one hour before scratching. After scratching, the cells were incubated with 10 µM (+)-PTZ or vehicle for five hours. (**A**) Representative images show the original scratch (day 0), and migration of WT ONHAs into the wound area after five hours of incubation with (+)-PTZ treatment or vehicle control. *Scale bar*: 200 µm. (**B**) Wound distance was measured using ZEN software. The wound distance significantly decreased when WT ONHAs were treated with (+)-PTZ. Significantly different from control $^{**}P < 0.01$. The results were repeated in triplicate with cells isolated from different animals, on different dates, and treated on different days. (**C**) Representative images show cells stained with Arp3 antibody (*red*), phalloidin (*green*), and DAPI (*blue*). *Scale bar*: 50 µm. (**D**) Quantification of the number of lamellipodia for each cell. For each group, 100 cells, located at the wound edge, were quantified. (+)-PTZ treated cells had significantly more lamellipodia than control ONHAs. Significantly different from control $^{**}P < 0.01$. Data were analyzed using Student's *t*-test. The results were repeated in triplicate with cell cultures isolated from different animals, on different dates, and treated on different days.

the baseline migration of KO ONHAs is increased, (+)-PTZ does not stimulate KO ONHA migration.

Next, to better understand the time frame of S1R-stimulated ONHA migration and morphological changes, we performed migration assay at an early time point (5 hours after (+)-PTZ treatment) and labeled cells for the lamellipodial marker, Actin Related Protein 3 (Arp3). For the migration assay, cultured WT ONHAs were treated with 10 µM (+)-PTZ or vehicle (control) for one hour prior to scratch. Treatment with either (+)-PTZ or vehicle was continued for 5h following scratch. At the five-hour time point, astrocyte migration into the wound area was significantly increased in the (+)-PTZ treated WT cultures compared with vehicle treated control cultures (Figs. 5A, 5B). In addition, immunohistochemical evaluation showed an increased number of Arp3-labeled lamellipodia in (+)-PTZ–treated cultures compared with vehicle-treated controls (Figs. 5C, 5D).

To evaluate responses of ONHAs under conditions of ischemic cellular stress, we subjected WT-derived primary cell cultures to oxygen-glucose deprivation (OGD). After six hours of OGD, we then exposed the cells to resumption of normoxia (reperfusion) for a time period of 18 hours (OGD/R). Using immunocytochemistry, we measured GFAP levels in both OGD/R-exposed, and normoxic cultures (Fig. 6A). We then treated ONHAs with (+)-PTZ for one hour before OGD/R. In Figure 6A, we show representative images from control (normoxic), OGD/R-exposed, and (+)-PTZ–treated + OGD/R-exposed cell cultures. Quantitative analysis of immunocytochemistry showed that OGD/R exposure increased GFAP levels (Fig. 6B). In addition, analyses indicated that (+)-PTZ treatment of OGD/R-exposed cell cultures significantly enhanced the OGD/R-induced increase in GFAP levels (Fig. 6B). In addition to measurement of GFAP, we used MTT assay to measure cell proliferation

Investigative Ophthalmology & Visual Science

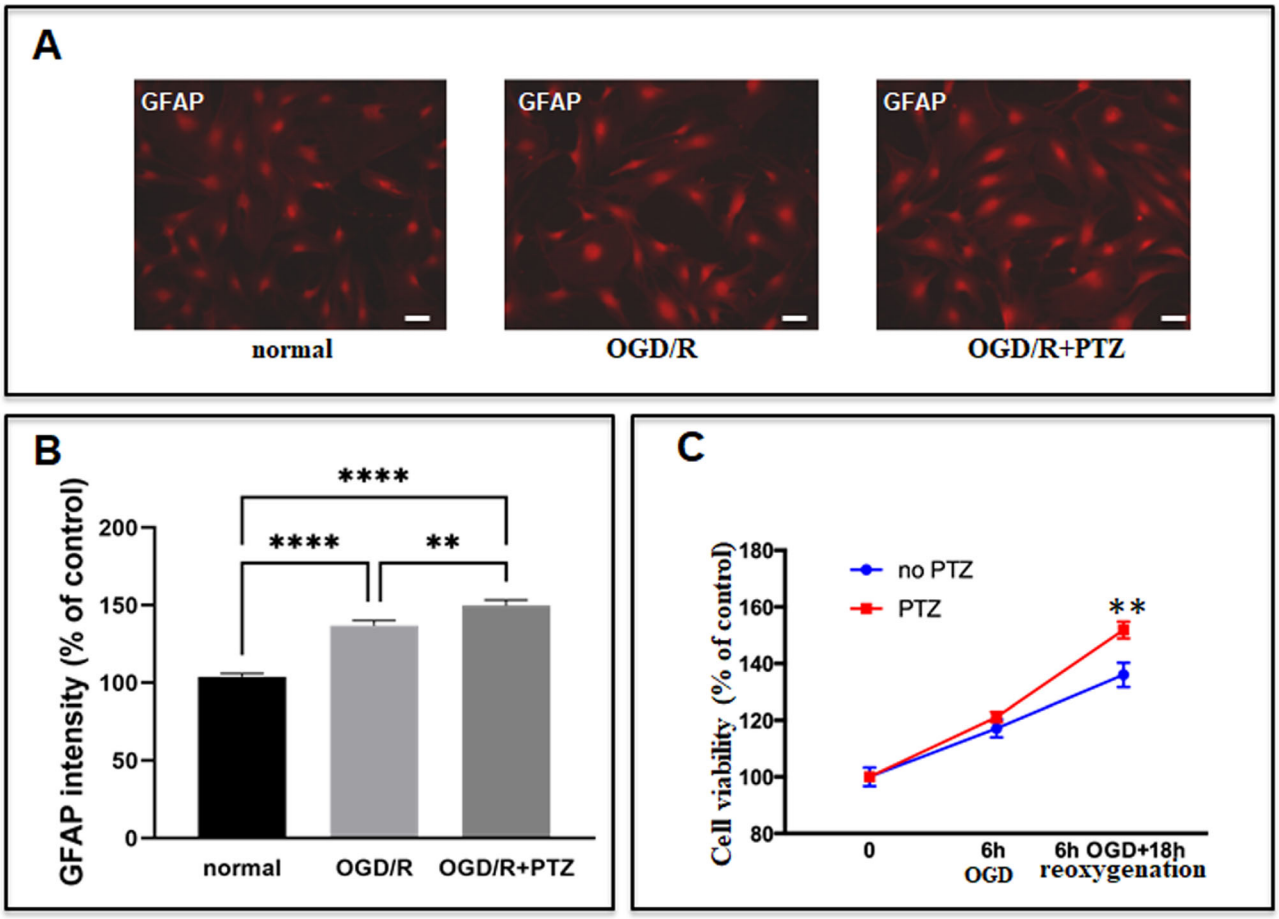

Figure 6. Effect of (+)-PTZ treatment on OGD/R-exposed WT ONHAs. (**A**) Representative images show GFAP expression in WT ONHAs under normal and OGD/R-exposed conditions, with or without (+)-PTZ treatment. *Scale bar*: 50 µm. (**B**) Quantitative analysis shows that OGD/R increases GFAP expression, and that (+)-PTZ treatment enhances the OGD/R-induced increase in GFAP expression. Significantly different from control $^{****}P < 0.0001$, $^{**}P < 0.01$. (**C**) Cell proliferation was detected by MTT assay. Under conditions of OGD/R exposure, (+)-PTZ treated cells showed a higher proliferation rate than non-(+)-PTZ treated cells. Significantly different from control $^{**}P < 0.01$. Data were analyzed using two-way ANOVA followed by Tukey-Kramer post-hoc test for multiple comparisons. These experiments were repeated in triplicate with cells isolated from different dates, different animals and treated on different days. For each group of each isolation, three coverslips were quantified.

under conditions of OGD/R. As represented in Figure 6C, astrocytes subjected to OGD/R showed increased cellular proliferation compared with normoxic (control) cultures. Furthermore, (+)-PTZ treatment of ONHAs significantly augmented the OGD/R-induced increase in astrocyte proliferation (Fig. 6C).

We also evaluated responses of KO-derived ONHAs under conditions of OGD/R, and in the presence and absence of treatment with (+)-PTZ (Figs. 7A–7C). Figure 7A shows representative images of immunocytochemical labeling for GFAP in KO cultures derived under control (normoxic), OGD/R-exposed, and (+)-PTZ–treated + OGD/R-exposed conditions. Similar to evaluation of WT cell cultures, quantitative assessment of GFAP in KO cultures showed an OGD-induced increase in GFAP levels (Fig. 7B). In contrast to WT ONHAs, (+)-PTZ treatment of KO ONHAs did not cause significant GFAP enhancement (Figure 7B). We also evaluated cell proliferation in KO-derived cultures using MTT assay. Results, presented in Figure 7C, were consistent with assessment of WT cultures. The assessment showed increased cellular proliferation under conditions of OGD/R compared with normoxic (control) conditions. However, in contrast to WT ONHAs, KO ONHAs did not show significantly augmented cellular proliferation when treated with (+)-PTZ.

In addition to effects on GFAP levels and cellular proliferation, ischemic conditions may influence astrocyte migration.[50] We evaluated the effects of OGD/R on ONHA migration in WT and S1R KO ONHAs, and in the presence and absence of treatment with (+)-PTZ. Figure 8 shows representative images. First, we compared cellular migration into the wounded area for WT OGD/R-exposed astrocytes versus WT normoxic (control) cultures. Results showed no significant OGD/R-induced change in WT astrocyte migration (Figs. 8A, 8B). We then evaluated cellular migration in OGD/R-exposed WT ONHAs under conditions of treatment with (+)-PTZ. The (+)-PTZ–treated, WT OGD/R-exposed ONHAs showed increased cellular migration into the wound area compared with WT OGD/R-exposed, nontreated cultures (Figs. 8A, 8B). Next, we measured cellular migration for KO ONHAs under conditions of OGD/R. In contrast to WT-derived cultures, OGD/R-exposed KO ONHAs showed significantly decreased migration into the wound area compared with KO normoxic (control) cultures. Finally, we

Investigative Ophthalmology & Visual Science

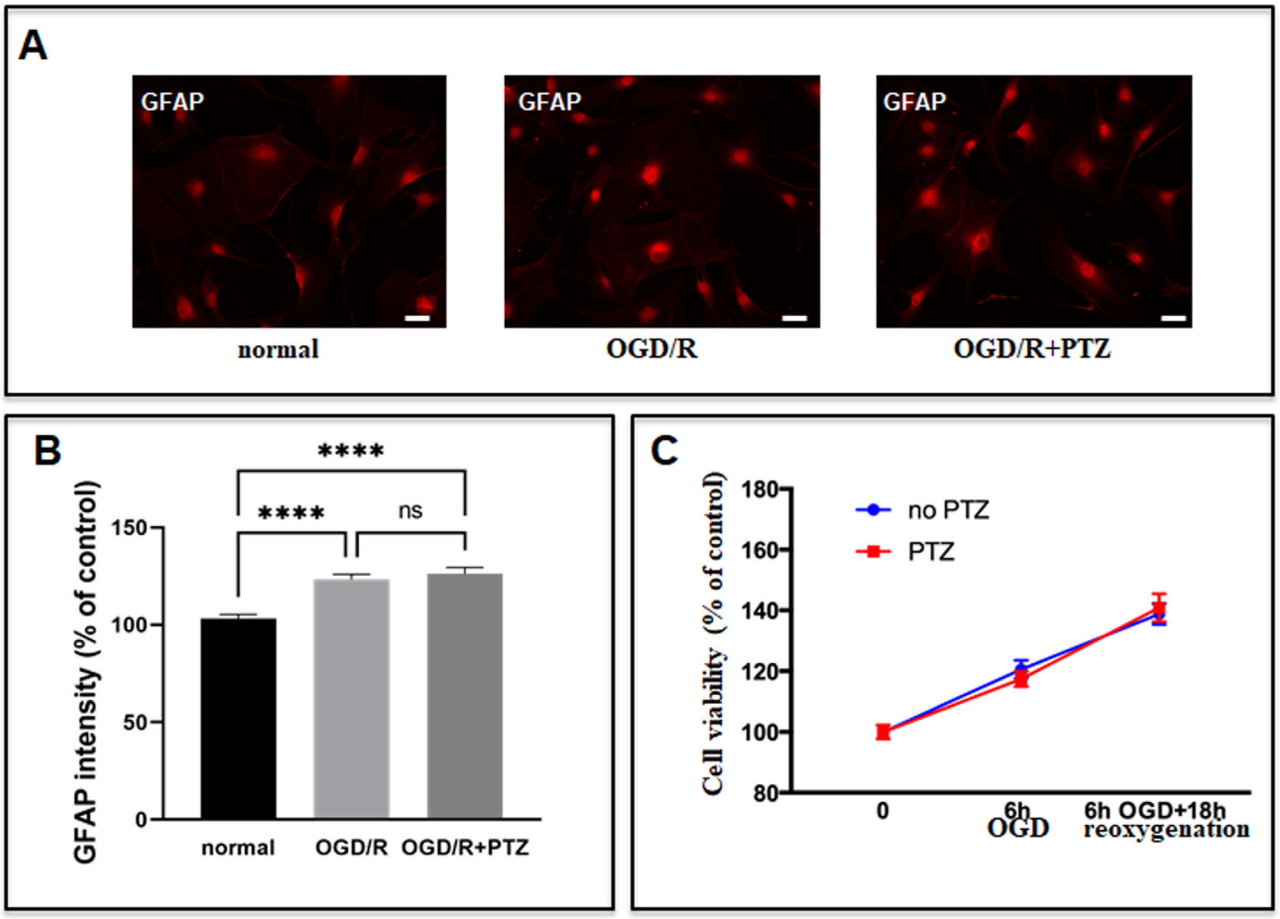

Figure 7. Effect of (+)-PTZ treatment on OGD/R-exposed S1R KO ONHAs. (**A**) Representative images show GFAP expression in S1R KO ONHAs under normal and OGD/R-exposed conditions with or without (+)-PTZ treatment. *Scale bar*: 50 µm. (B) Quantitative analysis shows that OGD/R increases GFAP expression, and that (+)-PTZ treatment does not significantly enhance the OGD/R-induced increase in GFAP expression. Significantly different from control $^{****}P < 0.0001$, $^{***}P < 0.001$, $^{*}P < 0.05$. (**C**) Cell proliferation was detected by MTT assay. Under conditions of OGD/R exposure, (+)-PTZ treatment did not significantly affect the S1R KO ONHA proliferation rate. Data were analyzed using two-way ANOVA followed by Tukey-Kramer post hoc test for multiple comparisons. These experiments were repeated in triplicate with cells isolated from different dates, different animals and treated on different days. For each group of each isolation, three coverslips were quantified.

evaluated cellular migration in OGD/R-exposed KO ONHAs under conditions of treatment with (+)-PTZ. The (+)-PTZ–induced increase in ONHA migration observed in OGD/R-exposed WT ONHAs was not observed for S1R KO ONHAs (Figs. 8A, 8C).

To evaluate the effects of S1R stimulation on pathways that regulate astrocytic reactivity, we measured activation of signaling molecules, STAT3 and NFkB. Astrocytes in the optic nerve, brain and spinal cord express STAT3 and NFkB, and both molecules are activated via phosphorylation under conditions of neuronal tissue injury due to ischemia, inflammation, and neurodegenerative disease states.[51–56] Therefore we measured phosphorylation levels of STAT3 (p-STAT3) and the p65 subunit of NFkB(p-p65). To do this, we derived cellular lysates from (+)-PTZ–treated versus nontreated ONHA cultures under conditions of normoxia and OGD/R. Lysates were analyzed by western blot, and probed with antibodies to p-STAT3 and p-p65. Under normoxic conditions, treatment of WT ONHAs with (+)-PTZ did not change levels of p-STAT3 or p-65 (Figs. 9A–9C). Exposure of WT ONHAs to OGD/R resulted in elevated levels of pSTAT3 that were enhanced by (+)-PTZ treatment (Figs. 9A–9C). In contrast, although p-p65 levels were increased by ONHA exposure to OGD/R, treatment with (+)-PTZ abrogated the OGD/R-induced rise in p-p65 levels (Figs. 9A–9C).

We also used Western blot analysis to measure S1R levels under conditions of OGD/R versus normoxia and in the presence and absence of treatment with (+)-PTZ. Lysates derived from OGD/R-exposed ONHAs showed increased S1R levels compared with lysates derived from normoxic cultures. S1R levels were not significantly changed by treatment with (+)-PTZ in either OGD/R-exposed or normoxic ONHA cell cultures (Figs. 9A, 9D).

Discussion

Our results indicate that S1R plays a role in regulation of the reactivity responses of ONH-derived astrocytes in cell culture under ischemic conditions. Astrocyte reactivity responses include cellular migration, proliferation, upregulation of GFAP levels, reorganization of actin networks, and changes in intracellular signaling and regulatory pathways.

Our previous studies, carried out using ONHAs derived from neonatal rat pups, showed that S1R activation prevents

Investigative Ophthalmology & Visual Science

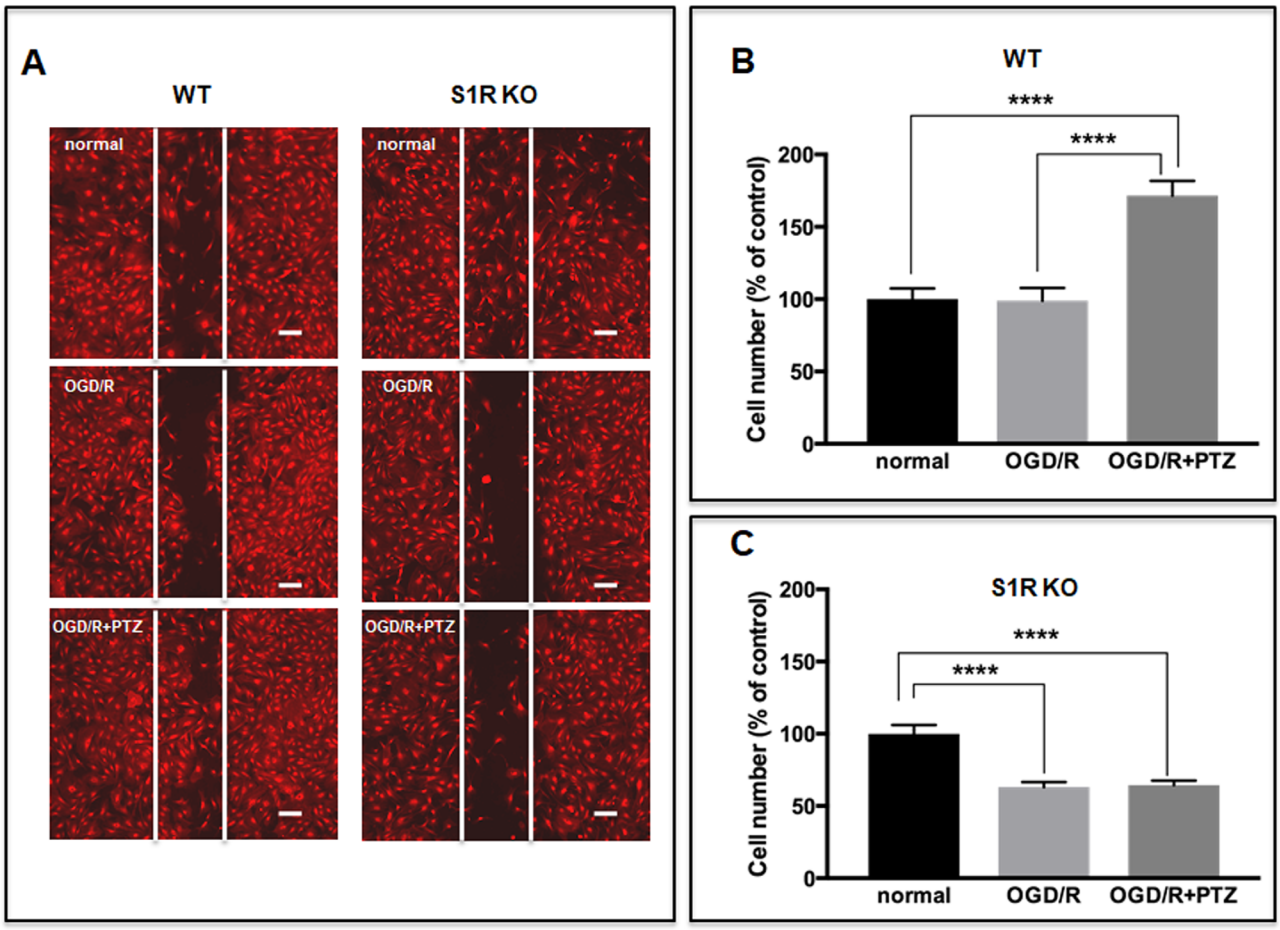

Figure 8. Effect of (+)-PTZ on migration of OGD/R-exposed ONHAs. Both WT and S1R KO ONHAs were pretreated with 10 µM (+)-PTZ for one hour before scratching. After scratching, the cells were incubated with 10 µM (+)-PTZ under OGD for six hours, followed by reoxygenation for 18 hours. (**A**) Representative images show migration of WT versus S1R KO normoxic (control) and OGD/R-exposed cells into the wounded area with or without (+)-PTZ treatment. *Scale bar*: 200 µm. (**B**) Cells in wounded area were counted by ImageJ. For each group, four coverslips were quantified. WT ONHA migration increased when cells were treated with (+)-PTZ after OGD/R. Significantly different from control ****$P < 0.0001$. S1R KO ONHA migration was not affected by (+)-PTZ treatment. Data were analyzed using one-way ANOVA followed by Tukey-Kramer post hoc test for multiple comparisons. Experiments were repeated in triplicates with cells isolated from different dates, different animals and treated on different days. For each group of each isolation, three coverslips were quantified.

intracellular reactive oxygen species generation and oxidative stress-induced cell death.[46] The current study examines reactivity responses of ONHAs cultured from adult mice. The prevalence of most neurodegenerative conditions, including optic neuropathies, increases with age.[57,58] Therefore cultures derived from adult animals likely represent a better pathophysiological model system for age-related conditions than those derived from neonatal animals. In addition, expansion of our ONHA culture system for use in mice allows for evaluation of astrocytes derived from S1R KO mice. Furthermore, neonatal astrocytic tissues are more plastic and labile to stimuli than adult astrocytes, so adult-derived cultures may respond more reliably to reactivity-inducing cellular stress.[59]

As shown in Figures 4 and 5, under conditions of scratch-wound assay, we found a significant increase in ONHA migration in WT, non-stressed, (+)-PTZ pre-treated cells compared to WT, non-stressed, no (+)-PTZ treatment controls at both 24h and 5h time points following scratch. Consistent with our results, Wang et al.[60] found increased cellular migration upon stimulation of astrocytes with the S1R agonist, (+)SKF-10047.

We also compared GFAP levels and cellular migration in nonstressed ONHAs derived from S1R KO mice to cultures derived from WT mice. Interestingly, our results (Figs. 3 and 4) showed that KO ONHAs expressed higher GFAP levels and showed increased baseline migration response compared with cultures derived from WT mice. These results are consistent with those reported by Weng et al.,[61] showing increased GFAP levels in primary neuron-astrocyte co-cultures derived from S1R KO murine brain. Astrocytes play critical roles in neuronal homeostasis, and compensatory astrocyte reactivity occurs throughout the CNS under conditions of neuronal injury or stress.[62] It is well known that S1R-mediated cellular functions are associated with the pathogenesis of neurodegenerative disorders.[63] Baseline GFAP elevation in ONHAs isolated from S1R KO animals may result from compensatory neuron-glial interactions initiated within the S1R-lacking optic nerve prior to astrocyte isolation. Similar cellular counterbalances may occur within brains of

Investigative Ophthalmology & Visual Science

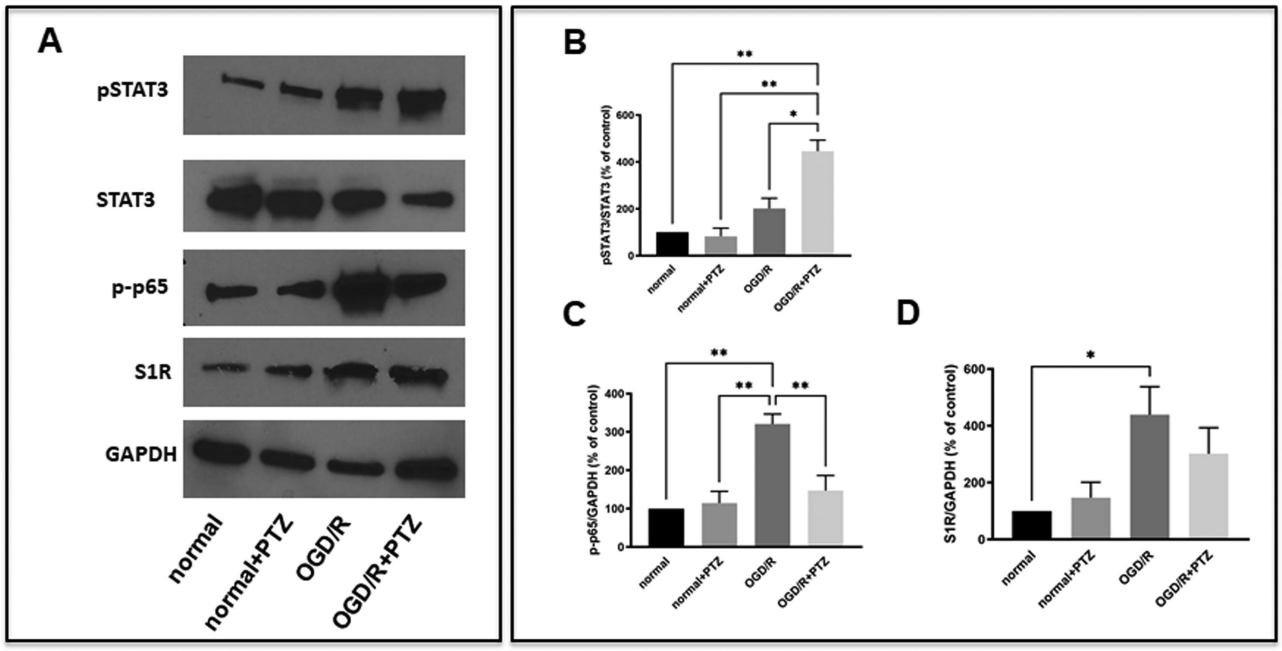

Figure 9. Effect of (+)-PTZ on phosphorylation of STAT3 and NFkB p-65 in WT ONHAs. (**A**) Representative Western blot showing increased phosphorylation of both STAT3 and NFkB p-65 after OGD/R in WT ONHAs. (+)-PTZ treatment enhanced OGD/R-induced STAT-3 phosphorylation, whereas (+)-PTZ treatment abrogated OGD/R-induced phosphorylation of p-65. In addition, S1R expression was increased under OGD/R exposure. (**B–D**) Quantitative analysis by ImageJ. Significantly different from control $^{**}P < 0.01$, $^{*}P < 0.05$. Data were analyzed using one-way ANOVA followed by Tukey-Kramer for multiple comparisons. These experiments were repeated in triplicate with cells isolated from different dates, different animals and treated on different days.

S1R KO mice and lead to increased GFAP levels in mixed astrocyte-neuronal cultures as described by Weng et al.[61] Further studies of how S1R mediates cooperation between neurons and glia under conditions of neuronal stress, and within specific regions of the brain and spinal cord are warranted.

An additional key feature of our studies is evaluation of ONHAs under conditions of oxygen-glucose deprivation and recovery. Optic nerve ischemia has been implicated in acute and chronic optic neuropathies.[64] Therefore responses of ONHAs to transient ischemic insult may be relevant to several optic neuropathies, including nonarteritic ischemic optic neuropathy and glaucoma.[65]

Our preliminary evaluation in WT ONHAs indicated that six hours of OGD exposure, followed by 18 hours of normoxia caused a significant increase in intracellular GFAP levels (Fig. 6). Consistent with our observations, previous studies of brain-derived astrocytes found an increase, or spike, in GFAP levels upon normoxic recovery from OGD.[66,67]

Interestingly, our results showed that (+)-PTZ treatment of OGD/R-exposed WT ONHAs led to enhancement of astrocyte reactivity measures, including increased GFAP levels, and augmentation of cellular proliferation and migration (Figs. 6 and 8). The (+)-PTZ–mediated enhancement of reactivity responses was absent in OGD/R-exposed ONHAs derived from S1R KO mice (Figs. 7 and 8). These observations of S1R KO-derived ONHAs lead to the conclusion that (+)-PTZ–mediated effects on OGD/R-induced astrocyte reactivity are dependent on S1R.

Consistent with our results, recent studies in brain and spinal cord indicate that S1Rs modulate aspects of astrocyte reactivity.[60,68] Our studies also aimed to evaluate the effects of S1R stimulation on upstream pathways that regulate astrocytic reactivity. Therefore we measured activation of signaling molecules, STAT3 and NFkB. STAT3 is a critical regulator of astrocyte reactivity and is expressed within astrocytes in the brain, spinal cord and optic nerve.[51,65,69–71] In the brain, spinal cord, and optic nerve, conditional KO of STAT3 from astrocytes attenuates GFAP upregulation and astrocytic scar formation.[12,72–74] In several models, this reduction in astrocyte reactivity leads to exacerbation of neuronal damage. In the optic nerve, attenuation of astrocyte reactivity through conditional STAT3 KO causes increased loss of RGCs and visual function under conditions of glaucomatous stress.[12] Therefore STAT3 activation within the optic nerve head may play a protective role in supporting the health of RGCs under stressful conditions.

Similar to STAT3, the NFkB transcription factor regulates cellular response to stress.[75,76] However, in contrast to STAT3, multiple studies suggest that astrocytic activation of NFkB promotes neuronal damage in ischemic, inflammatory, and traumatic circumstances.[56,77] For example, astrocyte-specific transgenic inhibition of NFkB within the optic nerve protects RGCs under conditions of experimental optic neuritis.[78]

Our studies indicate that exposure of ONHAs to OGD/R leads to increased phosphorylation of both STAT3 and the p65 subunit of NFkB (Fig. 9). Therefore, according to our observations, both STAT3 and NFkB are activated in ONHA cultures under conditions of OGD/R. Interestingly, we find that (+)-PTZ–mediated stimulation of S1R enhances the OGD/R-induced STAT3 activation (Fig. 9). In contrast, we find that (+)-PTZ–mediated S1R stimulation mitigates the OGD/R-induced NFkB (p-65) activation (Fig. 9). Given previous studies of the roles of STAT3 and NFkB in

astrocytic injury and stress response, additional in vivo experiments are needed to determine whether S1R activation within ONHAs enhances the neuroprotective characteristics of these cells.

Previous studies indicate that (+)-PTZ–mediated activation of S1R can protect purified primary RGC cultures from death under conditions of OGD, as well as metabolic and excitotoxic stress.[43,45,79] Our studies elucidate a previously unknown mechanistic link between stimulation of S1R within ONHAs and the reactivity responses of these cells under conditions of ischemia-induced stress. Future studies, perhaps using ONHA-RGC cocultures, should address whether S1R-mediated activation of ONHAs is protective of RGCs independent of S1R stimulation within the RGCs themselves.

Acknowledgments

Supported by the National Institutes of Health (KEB:R01EY027406 SBS: R01EY028103, and Center core grant for vision research (P30) P30 EY031631), and the American Glaucoma Society.

Disclosure: **J. Zhao,** None; **G. Gonsalvez,** None; **M. Bartoli,** None; **B.A. Mysona,** None; **S.B. Smith,** None; **K.E. Bollinger,** None

References

1. Quigley HA, Addicks EM, Green WR, Maumenee AE. Optic nerve damage in human glaucoma. II. The site of injury and susceptibility to damage. *Arch Ophthalmol.* 1981;99:635–649.
2. Quigley HA, Hohman RM, Addicks EM, Massof RW, Green WR. Morphologic changes in the lamina cribrosa correlated with neural loss in open-angle glaucoma. *Am J Ophthalmol.* 1983;95:673–691.
3. Tham YC, Li X, Wong TY, Quigley HA, Aung T, Cheng CY. Global prevalence of glaucoma and projections of glaucoma burden through 2040: a systematic review and meta-analysis. *Ophthalmology.* 2014;121:2081–2090.
4. Wang R, Seifert P, Jakobs TC. Astrocytes in the optic nerve head of glaucomatous mice display a characteristic reactive phenotype. *Invest Ophthalmol Vis Sci.* 2017;58:924–932.
5. Tehrani S, Davis L, Cepurna WO, et al. Astrocyte structural and molecular response to elevated intraocular pressure occurs rapidly and precedes axonal tubulin rearrangement within the optic nerve head in a rat model. *Plos One.* 2016;11:e0167364.
6. Tehrani S, Davis L, Cepurna WO, et al. Optic nerve head astrocytes display axon-dependent and -independent reactivity in response to acutely elevated intraocular pressure. *Invest Ophthalmol Vis Sci.* 2019;60:312–321.
7. Hernandez MR, Wang N, Hanley NM, Neufeld AH. Localization of collagen types I and IV mRNAs in human optic nerve head by in situ hybridization. *Invest Ophthalmol Vis Sci.* 1991;32:2169–2177.
8. Johnson EC, Doser TA, Cepurna WO, et al. Cell proliferation and interleukin-6-type cytokine signaling are implicated by gene expression responses in early optic nerve head injury in rat glaucoma. *Invest Ophthalmol Vis Sci.* 2011;52:504–518.
9. Johnson EC, Jia L, Cepurna WO, Doser TA, Morrison JC. Global changes in optic nerve head gene expression after exposure to elevated intraocular pressure in a rat glaucoma model. *Invest Ophthalmol Vis Sci.* 2007;48:3161–3177.
10. Lye-Barthel M, Sun D, Jakobs TC. Morphology of astrocytes in a glaucomatous optic nerve. *Invest Ophthalmol Vis Sci.* 2013;54:909–917.
11. Johnson EC, Morrison JC. Friend or foe? Resolving the impact of glial responses in glaucoma. *J Glaucoma.* 2009;18:341–353.
12. Sun D, Moore S, Jakobs TC. Optic nerve astrocyte reactivity protects function in experimental glaucoma and other nerve injuries. *J Exp Med.* 2017;214:1411–1430.
13. Iwase A, Suzuki Y, Araie M, et al. The prevalence of primary open-angle glaucoma in Japanese: the Tajimi Study. *Ophthalmology.* 2004;111:1641–1648.
14. Heijl A, Leske MC, Bengtsson B, et al. Reduction of intraocular pressure and glaucoma progression: results from the Early Manifest Glaucoma Trial. *Arch Ophthalmol.* 2002;120:1268–1279.
15. Kass MA, Heuer DK, Higginbotham EJ, et al. The Ocular Hypertension Treatment Study: a randomized trial determines that topical ocular hypotensive medication delays or prevents the onset of primary open-angle glaucoma. *Arch Ophthalmol.* 2002;120:701–713; discussion 829–730.
16. Kerr J, Nelson P, O'Brien C. A comparison of ocular blood flow in untreated primary open-angle glaucoma and ocular hypertension. *Am J Ophthalmol.* 1998;126:42–51.
17. Arend O, Plange N, Sponsel WE, Remky A. Pathogenetic aspects of the glaucomatous optic neuropathy: fluorescein angiographic findings in patients with primary open angle glaucoma. *Brain Res Bull.* 2004;62:517–524.
18. Fuchsjager-Mayrl G, Wally B, Georgopoulos M, et al. Ocular blood flow and systemic blood pressure in patients with primary open-angle glaucoma and ocular hypertension. *Invest Ophthalmol Vis Sci.* 2004;45:834–839.
19. Lafuente MP, Villegas-Perez MP, Selles-Navarro I, Mayor-Torroglosa S, Miralles de Imperial J, Vidal-Sanz M. Retinal ganglion cell death after acute retinal ischemia is an ongoing process whose severity and duration depends on the duration of the insult. *Neuroscience.* 2002;109:157–168.
20. Joo CK, Choi JS, Ko HW, et al. Necrosis and apoptosis after retinal ischemia: involvement of NMDA-mediated excitotoxicity and p53. *Invest Ophthalmol Vis Sci.* 1999;40:713–720.
21. Wang L, Cull G, Burgoyne CF, Thompson S, Fortune B. Longitudinal alterations in the dynamic autoregulation of optic nerve head blood flow revealed in experimental glaucoma. *Invest Ophthalmol Vis Sci.* 2014;55:3509–3516.
22. Cull G, Burgoyne CF, Fortune B, Wang L. Longitudinal hemodynamic changes within the optic nerve head in experimental glaucoma. *Invest Ophthalmol Vis Sci.* 2013;54:4271–4277.
23. Yu AL, Fuchshofer R, Birke M, et al. Hypoxia/reoxygenation and TGF-beta increase alphaB-crystallin expression in human optic nerve head astrocytes. *Exp Eye Res.* 2007;84:694–706.
24. Alonso G, Phan V, Guillemain I, et al. Immunocytochemical localization of the sigma(1) receptor in the adult rat central nervous system. *Neuroscience.* 2000;97:155–170.
25. Mavlyutov TA, Epstein M, Guo LW. Subcellular localization of the sigma-1 receptor in retinal neurons - an electron microscopy study. *Sci Rep.* 2015;5:10689.
26. Ola MS, Moore P, El-Sherbeny A, et al. Expression pattern of sigma receptor 1 mRNA and protein in mammalian retina. *Brain Res Mol Brain Res.* 2001;95:86–95.
27. Mavlyutov TA, Epstein ML, Verbny YI, et al. Lack of sigma-1 receptor exacerbates ALS progression in mice. *Neuroscience.* 2013;240:129–134.
28. Mavlyutov TA, Guo LW, Epstein ML, Ruoho AE. Role of the Sigma-1 receptor in Amyotrophic Lateral Sclerosis (ALS). *J Pharmacol Sci.* 2015;127:10–16.
29. Nguyen L, Lucke-Wold BP, Mookerjee SA, et al. Role of sigma-1 receptors in neurodegenerative diseases. *J Pharmacol Sci.* 2015;127:17–29.

30. Ruscher K, Inacio AR, Valind K, Rowshan Ravan A, Kuric E, Wieloch T. Effects of the sigma-1 receptor agonist 1-(3,4-dimethoxyphenethyl)-4-(3-phenylpropyl)-piperazine dihydro-chloride on inflammation after stroke. *Plos One.* 2012;7:e45118.
31. Shen YC, Wang YH, Chou YC, et al. Dimemorfan protects rats against ischemic stroke through activation of sigma-1 receptor-mediated mechanisms by decreasing glutamate accumulation. *J Neurochem.* 2008;104:558–572.
32. Mavlyutov TA, Guo LW. Peeking into sigma-1 receptor functions through the retina. *Adv Exp Med Biol.* 2017;964:285–297.
33. Bucolo C, Drago F, Lin LR, Reddy VN. Sigma receptor ligands protect human retinal cells against oxidative stress. *Neuroreport.* 2006;17:287–291.
34. Ola MS, Moore P, Maddox D, et al. Analysis of sigma receptor (sigmaR1) expression in retinal ganglion cells cultured under hyperglycemic conditions and in diabetic mice. *Brain Res Mol Brain Res.* 2002;107:97–107.
35. Smith SB, Duplantier J, Dun Y, et al. In vivo protection against retinal neurodegeneration by sigma receptor 1 ligand (+)-pentazocine. *Invest Ophthalmol Vis Sci.* 2008;49:4154–4161.
36. Zhao J, Mysona BA, Qureshi A, et al. (+)-Pentazocine reduces NMDA-induced murine retinal ganglion cell death through a sigmaR1-dependent mechanism. *Invest Ophthalmol Vis Sci.* 2016;57:453–461.
37. Zhao L, Chen G, Li J, et al. An intraocular drug delivery system using targeted nanocarriers attenuates retinal ganglion cell degeneration. *J Control Release.* 2017;247:153–166.
38. Wang J, Saul A, Roon P, Smith SB. Activation of the molecular chaperone, sigma 1 receptor, preserves cone function in a murine model of inherited retinal degeneration. *Proc Natl Acad Sci USA.* 2016;113:E3764–E3772.
39. Shimazawa M, Sugitani S, Inoue Y, Tsuruma K, Hara H. Effect of a sigma-1 receptor agonist, cutamesine dihydrochloride (SA4503), on photoreceptor cell death against light-induced damage. *Exp Eye Res.* 2015;132:64–72.
40. Ha Y, Saul A, Tawfik A, et al. Late-onset inner retinal dysfunction in mice lacking sigma receptor 1 (sigmaR1). *Invest Ophthalmol Vis Sci.* 2011;52:7749–7760.
41. Sabino V, Cottone P, Parylak SL, Steardo L, Zorrilla EP. Sigma-1 receptor knockout mice display a depressive-like phenotype. *Behav Brain Res.* 2009;198:472–476.
42. Sha S, Hong J, Qu WJ, et al. Sex-related neurogenesis decrease in hippocampal dentate gyrus with depressive-like behaviors in sigma-1 receptor knockout mice. *Eur Neuropsychopharmacol.* 2015;25:1275–1286.
43. Dun Y, Thangaraju M, Prasad P, Ganapathy V, Smith SB. Prevention of excitotoxicity in primary retinal ganglion cells by (+)-pentazocine, a sigma receptor-1 specific ligand. *Invest Ophthalmol Vis Sci.* 2007;48:4785–4794.
44. Ha Y, Shanmugam AK, Markand S, Zorrilla E, Ganapathy V, Smith SB. Sigma receptor 1 modulates ER stress and Bcl2 in murine retina. *Cell Tissue Res.* 2014;356:15–27.
45. Mueller BH, 2nd, Park Y, Ma HY, et al. Sigma-1 receptor stimulation protects retinal ganglion cells from ischemia-like insult through the activation of extracellular-signal-regulated kinases 1/2. *Exp Eye Res.* 2014;128:156–169.
46. Zhao J, Mysona BA, Wang J, Gonsalvez GB, Smith SB, Bollinger KE. Sigma 1 receptor regulates ERK activation and promotes survival of optic nerve head astrocytes. *Plos One.* 2017;12:e0184421.
47. Wang J, Cui X, Roon P, Smith SB. Role of sigma 1 receptor in retinal degeneration of the Ins2Akita/+ murine model of diabetic retinopathy. *Invest Ophthalmol Vis Sci.* 2016;57:2770–2781.
48. Hol EM, Pekny M. Glial fibrillary acidic protein (GFAP) and the astrocyte intermediate filament system in diseases of the central nervous system. *Curr Opin Cell Biol.* 2015;32:121–130.
49. Sofroniew MV, Vinters HV. Astrocytes: biology and pathology. *Acta Neuropathol.* 2010;119:7–35.
50. Ou-Yang L, Liu Y, Wang BY, et al. Carnosine suppresses oxygen-glucose deprivation/recovery-induced proliferation and migration of reactive astrocytes of rats in vitro. *Acta Pharmacol Sin.* 2018;39:24–34.
51. Acarin L, Gonzalez B, Castellano B. STAT3 and NFkappaB activation precedes glial reactivity in the excitotoxically injured young cortex but not in the corresponding distal thalamic nuclei. *J Neuropathol Exp Neurol.* 2000;59:151–163.
52. Justicia C, Gabriel C, Planas AM. Activation of the JAK/STAT pathway following transient focal cerebral ischemia: Signaling through Jak1 and Stat3 in astrocytes. *Glia.* 2000;30:253–270.
53. Sriram K, Benkovic SA, Hebert MA, Miller DB, O'Callaghan JP. Induction of gp130-related cytokines and activation of JAK2/STAT3 pathway in astrocytes precedes up-regulation of glial fibrillary acidic protein in the 1-methyl-4-phenyl-1,2,3,6-tetrahydropyridine model of neurodegeneration - Key signaling pathway for astrogliosis in vivo? *J Biol Chem.* 2004;279:19936–19947.
54. Yamauchi K, Osuka K, Takayasu M, et al. Activation of JAK/STAT signalling in neurons following spinal cord injury in mice. *J Neurochem.* 2006;96:1060–1070.
55. Zhang SD, Li WY, Wang WQ, Zhang SS, Huang P, Zhang C. Expression and Activation of STAT3 in the Astrocytes of Optic Nerve in a Rat Model of Transient Intraocular Hypertension. *Plos One* 2013;8(1):e55683.
56. Agapova OA, Kaufman PL, Hernandez MR. Androgen receptor and NFkB expression in human normal and glaucomatous optic nerve head astrocytes in vitro and in experimental glaucoma. *Exp Eye Res.* 2006;82:1053–1059.
57. Guedes G, Tsai JC, Loewen NA. Glaucoma and aging. *Curr Aging Sci.* 2011;4:110–117.
58. Maresova P, Hruska J, Klimova B, Barakovic S, Krejcar O. Activities of Daily Living and Associated Costs in the Most Widespread Neurodegenerative Diseases: A Systematic Review. *Clin Interv Aging.* 2020;15:1841–1862.
59. Souza DG, Bellaver B, Souza DO, Quincozes-Santos A. Characterization of adult rat astrocyte cultures. *Plos One.* 2013;8(3):e60282.
60. Wang Y, Jiang HF, Ni J, Guo L. Pharmacological stimulation of sigma-1 receptor promotes activation of astrocyte via ERK1/2 and GSK3beta signaling pathway. *Naunyn Schmiedebergs Arch Pharmacol.* 2019;392:801–812.
61. Weng TY, Hung DT, Su TP, Tsai SA. Loss of Sigma-1 Receptor Chaperone Promotes Astrocytosis and Enhances the Nrf2 Antioxidant Defense. *Oxid Med Cell Longev.* 2017;2017:4582135.
62. Liddelow SA, Barres BA. Reactive astrocytes: production, function, and therapeutic potential. *Immunity.* 2017;46:957–967.
63. Ruscher K, Wieloch T. The involvement of the sigma-1 receptor in neurodegeneration and neurorestoration. *J Pharmacol Sci.* 2015;127:30–35.
64. Boke W, Voigt GJ. Circulatory disorders of the optic-nerve. *Ophthalmologica.* 1980;180:88–100.
65. Zhang S, Li W, Wang W, Zhang SS, Huang P, Zhang C. Expression and activation of STAT3 in the astrocytes of optic nerve in a rat model of transient intraocular hypertension. *Plos One* 2013;8:e55683.
66. Du LP, Mei ZG, Huang YG, et al. Protection of the Geum japonicum Thunb. var. chinense extracts against oxygen-glucose deprivation and re-oxygenation induced astrocytes

Investigative Ophthalmology & Visual Science

injury via BDNF/PI3K/Akt/CREB pathway. *Biomed Pharmacother.* 2020;127:110123.

67. Yang Q, Wang EY, Huang XJ, et al. Blocking epidermal growth factor receptor attenuates reactive astrogliosis through inhibiting cell cycle progression and protects against ischemic brain injury in rats. *J Neurochem.* 2011;119:644–653.
68. Zhang Y, Lv X, Bai Y, et al. Involvement of sigma-1 receptor in astrocyte activation induced by methamphetamine via up-regulation of its own expression. *J Neuroinflamm.* 2015;12:29.
69. Cattaneo E, Conti L, De-Fraja C. Signalling through the JAK-STAT pathway in the developing brain. *Trends Neurosci.* 1999;22:365–369.
70. Justicia C, Gabriel C, Planas AM. Activation of the JAK/STAT pathway following transient focal cerebral ischemia: signaling through Jak1 and Stat3 in astrocytes. *Glia.* 2000;30:253–270.
71. Yamauchi K, Osuka K, Takayasu M, et al. Activation of JAK/STAT signalling in neurons following spinal cord injury in mice. *J Neurochem.* 2006;96:1060–1070.
72. Okada S, Nakamura M, Katoh H, et al. Conditional ablation of Stat3 or Socs3 discloses a dual role for reactive astrocytes after spinal cord injury. *Nat Med.* 2006;12:829–834.
73. Haroon F, Drogemuller K, Handel U, et al. Gp130-dependent astrocytic survival is critical for the control of autoimmune central nervous system inflammation. *J Immunol.* 2011;186:6521–6531.
74. Wanner IB, Anderson MA, Song B, et al. Glial scar borders are formed by newly proliferated, elongated astrocytes that interact to corral inflammatory and fibrotic cells via STAT3-dependent mechanisms after spinal cord injury. *J Neurosci.* 2013;33:12870–12886.
75. Liu J, Du L. PERK pathway is involved in oxygen-glucose-serum deprivation-induced NF-kB activation via ROS generation in spinal cord astrocytes. *Biochem Biophys Res Commun.* 2015;467:197–203.
76. Oeckinghaus A, Ghosh S. The NF-kappaB family of transcription factors and its regulation. *Cold Spring Harb Perspect Biol.* 2009;1:a000034.
77. O'Neill LA, Kaltschmidt C. NF-kappa B: a crucial transcription factor for glial and neuronal cell function. *Trends Neurosci.* 1997;20:252–258.
78. Brambilla R, Dvoriantchikova G, Barakat D, Ivanov D, Bethea JR, Shestopalov VI. Transgenic inhibition of astroglial NF-kappaB protects from optic nerve damage and retinal ganglion cell loss in experimental optic neuritis. *J Neuroinflammation.* 2012;9:213.
79. Martin PM, Ola MS, Agarwal N, Ganapathy V, Smith SB. The sigma receptor ligand (+)-pentazocine prevents apoptotic retinal ganglion cell death induced in vitro by homocysteine and glutamate. *Brain Res Mol Brain Res.* 2004;123:66–75.